Collapsing animals

1999 J. Phys. A: Math. Gen. 32 1567

(http://iopscience.iop.org/0305-4470/32/9/007)

J. Phys. A: Math. Gen. **32** (1999) 1567–1584. Printed in the UK PII: S0305-4470(99)98135-0

Collapsing animals

E J Janse van Rensburg†, E Orlandini‡ and M C Tesi§

† Department of Mathematics and Statistics, York University, Toronto, Ontario, Canada M3J 1P3
‡ CEA-Saclay, Service de Physique Théorique, F-91191 Gif-sur-Yvette Cedex, France
§ Université de Paris-Sud, Mathématiques Bât 425, 91405 Orsay Cedex, France

Received 6 October 1998

Abstract. Lattice animals with fugacities conjugate to the number of indepedent cycles, or to the number of nearest neighbour contacts, go through a collapse transition at a θ-point at a critical value of the fugacity. We examine the phase diagram of a model which includes both a cycle and a contact fugacity with Monte Carlo methods. Using an underlying cut-and-paste Metropolis algorithm for lattice animals, we implement in the first instance a multiple Markov chain simulation of collapsing animals to estimate the location of the collapse transitions and the values of the crossover exponents associated with these. Secondly, we use umbrella sampling to sample animals over a rectangle in the phase diagram to examine the structure of the phase diagram of these animals.

1. Introduction

The θ-transition in models of linear and branched polymers has received considerable attention over a period which spans several decades (Mazur and McCrackin 1968, Mazur and McIntyre 1975, Sun *et al* 1980, Sun 1990, Park *et al* 1992, Tesi *et al* 1996, Madras and Janse van Rensburg 1997). This transition is also called the *collapse transition* and it occurs when the polymer collapses from an expanded conformation in a good solvent to a compact conformation in a solvent of poor quality. Between these phases, there is an intermediate regime which exists only at the critical point (or θ-point). This regime is characterized by properties distinct from those of either the expanded or collapsed phases. The collapse of the polymer is usually best characterized by a change in its metric properties. The mean linear dimension of the branched polymer (as a function of its total mass, M) is expected to scale as M^{ν} in the expanded phase, where ν is the *metric exponent* (in two dimensions $\nu \approx 0.64$, see for example Janse van Rensburg and Madras (1997)). In the collapsed phase this scaling becomes $M^{1/d}$ in d dimensions. However, theoretical and numerical studies strongly suggest the existence of an intermediate metric scaling regime characterized by the metric exponent $\nu_t < \nu$ at the θ-point in a variety of different models (see, for example, De Gennes 1975, 1978, Derrida and Herrmann 1983, Dickman and Schieve 1984, 1986, Duplantier 1986, 1987, Saleur 1986, Coniglio *et al* 1987, Duplantier and Saleur 1987, Lam 1987, 1988, Chang and Shapir 1988, Gaunt and Flesia 1990, 1991, Flesia and Gaunt 1992, Madras and Janse van Rensburg 1997).

The phase diagram of collapsing lattice animals has also been studied. There are a number of (different) versions of this model. This is best explained by noting that a lattice animal is characterized by its *order* (the number of vertices), its *size* (the number of edges), its *cyclomatic index* (the number of cycles), the number of *contacts* (these are pairs of vertices in the animal which are adjacent in the lattice, but not in the animal), and the number of *solvent contacts* (the number of lattice edges with one endpoint in the animal). The metric collapse of animals

0305-4470/99/091567+18$19.50

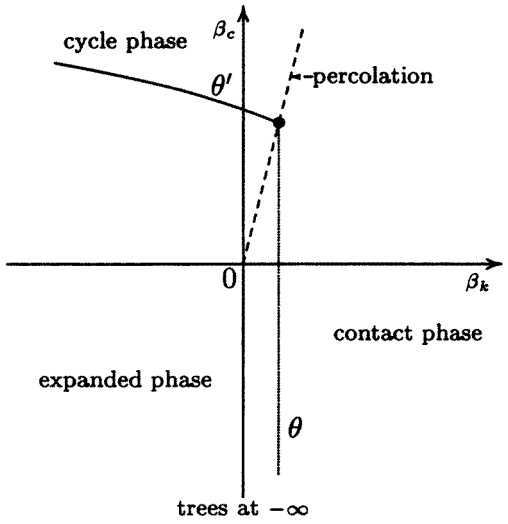

Figure 1. The phase diagram of lattice animals with a contact and a cycle fugacity. Critical percolation is marked with a •, and is on the intersection of a line of θ-transitions and a line along which animals are weighted as percolation clusters. The critical percolation point is a multicritical point which separates the critical line of θ-transitions into a line of tricritical collapse to a phase rich in contacts, and into a line of tricritical collapse into a phase rich in cycles.

in a particular model can be achieved by weighting the animals with respect either to the number of contacts (this is the k-model), or the cyclomatic index (this is the c-model, Derrida and Herrmann (1983)), or to the number of solvent contacts (this is the s-model, Flesia *et al* (1992a, b)). In each of these models the weighting is achieved by the introduction of a fugacity conjugate to the number of contacts, or conjugate to the number of cycles, and the collapse transition should occur at a critical value of the fugacity. The situation can be made even more interesting by the introduction of more than one fugacity (Flesia *et al* 1992a, b). In this paper we will consider the ck-model, where animals are counted with respect to their size and weighted with respect to the cyclomatic index and number of contacts. This model was studied in Janse van Rensburg and Madras (1997), where a cut-and-paste algorithm was developed and tested by calculating critical exponents associated with this model. The phase diagram of animals in this ensemble was also discussed, and is reproduced in figure 1. A curve of tricritical θ-points separates a phase of expanded animals (which includes the ensemble of uniformly weighted animals) from a phase of collapsed animals. This curve of θ-points contains the critical percolation point (where animals are weighted as percolation clusters), which divides it into two classes of collapse. In the first class there is a line of θ-points which is the result of a collapse due to an increasing contact fugacity, and the animals collapse to a phase of 'spanning tree' clusters. The second class is a curve of θ-points which is due to an increase in the cycle fugacity, and this collapse should be to a phase rich in cycles ('section graph' clusters). On the critical curve we find animals which are either critical with respect to collapse to spanning trees (called θ-animals), or critical with respect to collapse to section graphs (called θ'-animals). The possibility of a collapse–collapse transition between the collapse regime of 'section graph' clusters and 'spanning tree' clusters has been investigated in several studies. Although some evidence which supports the notion of such a transition was found by Flesia *et al* (1992a, b), Peard (1995), there is also no evidence for it in calculations based on the renormalization group and in a model of directed animals (Henkel and Seno 1996).

In this paper we investigate the phase diagram of collapsing animals as illustrated in figure 1. In particular, we consider an ensemble of animals of fixed size n on a square lattice, and we introduce fugacities conjugate to the number of cycles, and to the number of nearest neighbour contacts. In section 2 we discuss the phase diagram of this model, and various scaling hypotheses and their consequences are examined. We simulate animals in this ensemble by

using two separate and different Monte Carlo techniques (Metropolis *et al* 1953, Hammersley and Handscomb 1964). In the first place we use a multiple Markov chain implementation (see Geyer and Thompson 1994, Tesi *et al* 1996) of the algorithm discussed in Janse van Rensburg and Madras (1997) to study separately the collapse of animals with a contact fugacity and with a cycle fugacity. Secondly, we use umbrella sampling (Torrie and Valleau 1977, Valleau 1991, 1993a) techniques to accumulate data on a rectangle in the phase diagram which covers the expanded and the collapsed phases, as well as the curve of tricritical θ-points and the critical percolation point.

2. Collapsing animals

In this section we briefly review the hypothetical phase diagram and scaling in the ck-model of interacting animals. The partition function and free energy are first examined in section 2.1, and the phase diagram is discussed. Finite-size scaling and the scaling exponents are discussed in section 2.2.

2.1. The phase diagram

Let $a_n(c, k)$ be the number of lattice animals of n edges, c cycles and k nearest neighbour contacts. The partition function of this model is given by

$$Z_n(\beta_c, \beta_k) = \sum_{c,k} a_n(c, k) \mathrm{e}^{\beta_c c} \mathrm{e}^{\beta_k k} \tag{2.1}$$

where β_c is the *cycle fugacity*, and β_k is the *contact fugacity*. The limiting free energy of this model is known to exist (Janse van Rensburg and Madras, 1997):

$$\mathcal{F}(\beta_c, \beta_k) = \lim_{n\to\infty} \frac{1}{n} \log Z_n(\beta_c, \beta_k) \tag{2.2}$$

and $\mathcal{F}(\beta_c, \beta_k)$ is convex in both its arguments and is continuous, and differentiable almost everywhere.

In a lattice animal with n edges, c cycles and k contacts, s solvent contacts and v vertices it can be checked that

$$\begin{aligned} 1 &= v - n + c \\ 2dv &= 2n + 2k + s \end{aligned} \tag{2.3}$$

where d is the dimension of the lattice. We define the perimeter P of the animal as the number of nearest neighbour contacts and solvent contacts:

$$P = s + k. \tag{2.4}$$

It is possible to weight the animals in equation (2.1) such that it becomes a model of percolation clusters at a given probability p that an edge is open. In particular, the probability $P_n(p)$ that the cluster at the origin has size n edges is

$$P_n(p) = \sum_{c,k} a_n(c, k) v p^n (1 - p)^{s+k} \tag{2.5}$$

with $\{n, v, c, s, k\}$ related to each other as in equations (2.3) and (2.4). Eliminating v and s in equation (2.5) gives

$$P_n(p) = p^n (1 - p)^{2d+2(d-1)n} \sum_{c,k} (n + 1 - c) a_n(c, k) (1 - p)^{-2dc-k} \tag{2.6}$$

which is a weighted sum of the partition function in equation (2.1) and its derivatives, if

$$\beta_c = -2d \log(1 - p) \qquad d\beta_k = -\log(1 - p). \tag{2.7}$$

Thus, if the fugacities are related to p as in equation (2.7), then the model corresponds to percolation model at a probability p. In two dimensions the critical percolation probability is $p_c = \frac{1}{2}$, and we have critical percolation clusters at $(\beta_c^*, \beta_k^*) = (\log 16, \log 2)$. It is known that $P_\infty(p)$ (the percolation probability) is non-analytic at $p = p_c$ (Grimmett 1989), and so the point $(\log 16, \log 2)$ is also a non-analytic point of $\mathcal{F}(\beta_c, \beta_k)$. The rest of the phase diagram is expected to have the appearance proposed in figure 1. The percolation line intersects a curve of tricritical θ-transitions, presumably at the percolation point (since $P_\infty(p)$ is expected to be non-analytic only at this point). The percolation point divides the curve of θ-points into two critical curves of collapse transitions, each characterized by their own tricritical exponents. If β_c is fixed at a small or negative value, then presumably the collapse is into a phase poor in cycles and rich in nearest neighbour contacts. The tricritical exponents of this transition are expected to be those of a model of collapsing lattice trees, which is located at $\beta_c = -\infty$ in figure 1. We expect the collapsed animals to have the appearance of spanning trees in this collapsed regime, and we will refer to it as the *contact phase*. This transition is indicated by the line labelled by θ in figure 1. Numerical evidence suggest that this line of transitions may be a straight line. In particular, the location of the percolation point at $\beta_k^* = \log 2$, and the critical value of the nearest neighbour fugacity in lattice trees (estimated to be $\beta_k^t \approx 0.699 \pm 0.052$; see Janse van Rensburg and Madras (1996), Madras and Janse van Rensburg (1997)) strongly support this possibility. Similarly, if the contact fugacity β_k is kept small or negative, then the collapse is into a phase rich in cycles, this is the *cycle phase*. In this case, the transition should be related to the collapse of strongly embedded animals with a solvent or cycle fugacity (see Derrida and Hermann 1983)†. We indicate this collapse transition in figure 1 by the θ'-curve.

Another interesting issue presented by figure 1 is the following: are the line of θ-transition and the curve of θ'-transitions in the same universality class? Data collected in various studies (see Janse van Rensburg and Madras (1996), and Madras and Janse van Rensburg (1997) for details) suggest two different values of the crossover exponent along these lines. In this paper we aim to consider the points raised above. In particular, we are interested in the locations of the transitions, and in the values of the tricritical exponents associated with these.

2.2. Scaling

Specific heat. The finite-size free energy is defined by $F_n(\beta_c, \beta_k) = \frac{1}{n} \log Z_n(\beta_c, \beta_k)$. The usual finite-size scaling assumptions made for the free energy introduces the crossover exponents ϕ_c and ϕ_k, where we assume that ϕ_c describes the crossover to critical behaviour along the θ' curve with increasing n, and ϕ_k describes the crossover to critical behaviour along the θ-line. Therefore, if we are not close to the percolation point, where effects from both these lines may interfere to give a more complicated picture, we should expect that

$$F_n(\beta_c, \beta_k) \sim \begin{cases} \hat{f}(n^{\phi_k}\kappa)/n & \text{for contact collapse } (\theta\text{-line}) \\ \hat{g}(n^{\phi_c}\chi)/n & \text{for cycle collapse } (\theta'\text{-line}). \end{cases} \tag{2.8}$$

Here, κ and χ are scaling fields defined by $\kappa = (\beta_k^* - \beta_k)$ and $\chi = (\beta_c^* - \beta_c)$. The scaling functions $\hat{f}$ and $\hat{g}$ are assumed to approach constants if their arguments approach zero. The *specific heats* of the collapse transitions will be the most accessible quantity from a numerical point of view: these are the second derivatives of the free energy. Taking derivatives twice with respect to κ and to χ in equation (2.8) gives

$$C_n^{kk} \sim n^{2\phi_k - 1} \hat{f}''(n^{\phi_k}\kappa) \tag{2.9}$$

$$C_n^{cc} \sim n^{2\phi_c - 1} \hat{g}''(n^{\phi_c}\chi). \tag{2.10}$$

† Note that the model in this paper is different from that in the work by Derrida and Hermann (1983) where a model of strongly embedded lattice animals was considered.

The κ- and χ-dependence of these can be accentuated by the following manipulation of the right-hand sides of equations (2.9) and (2.10):

$$C_n^{kk} \sim n^{2\phi_k-1}\hat{f}''(n^{\phi_k}\kappa) \sim \kappa^{1/\phi_k-2}(n^{\phi_k}\kappa)^{2-1/\phi_k}\hat{f}''(n^{\phi_k}\kappa) \sim \kappa^{1/\phi_k-2}\hat{f}_0(n^{\phi_k}\kappa) \tag{2.11}$$

with $\hat{f}_0(x)$ defined in the obvious way, and a similar result is found for C_n^{cc}. The usual assumption that the singularity in the free energy is described by $\kappa^{2-\alpha_k}$, or by $\chi^{2-\alpha_c}$, where α_k and α_c are the *specific heat* exponents along the critical lines, then implies the hyperscaling relations:

$$2-\alpha_k = \frac{1}{\phi_k} \tag{2.12}$$

$$2-\alpha_c = \frac{1}{\phi_c}. \tag{2.13}$$

It is also possible to compute the Gaussian curvature of the free energy instead. Let

$$C_n^{kc} = \frac{\partial^2}{\partial\kappa\partial\chi}F_n(\beta_c,\beta_k) \tag{2.14}$$

then the Gaussian curvature is the Hessian of $F_n(\beta_c,\beta_k)$:

$$C_n^g = C_n^{kk}C_n^{cc} - C_n^{kc}C_n^{ck}. \tag{2.15}$$

Using equations (2.9) and (2.10), we conclude that

$$C_n^g \sim n^{2(\phi_c+\phi_k)-2} \tag{2.16}$$

close to the percolation point.

Metric scaling. In addition to the thermodynamic properties of animals as described above in terms of the specific heats, we shall also be interested in the metric behaviour of animals in the phase diagram in figure 1. Let $\langle R^2\rangle_n$ be the mean square radius of gyration. Then we expect

$$\langle R^2\rangle_n \sim \begin{cases} n^{2\nu} & \text{in the expanded phase} \\ n^{2\nu_\theta} & \text{along the } \theta\text{-line} \\ n^{2\nu_{\theta'}} & \text{along the } \theta'\text{-line} \\ n^{2\nu_p} & \text{at the critical percolation point.} \end{cases} \tag{2.17}$$

Available data (see for example, Derrida and Herrmann 1983, Janse van Rensburg and Madras 1996, Madras and Janse van Rensburg 1997) suggest that $\nu_\theta = \nu_{\theta'}$ along the critical curve, and that the value of the metric exponent at the percolation point (Stauffer 1979) is also equal to ν_θ. A more complete scaling assumption for the mean square radius of gyration will include a confluent correction, which is expressed by introducing a confluent exponent Δ:

$$\langle R^2\rangle_n = An^{2\nu}(1+Bn^{-\Delta}). \tag{2.18}$$

This scaling assumption is useful if we consider amplitude ratios involving $\langle R^2\rangle_n$. In particular, the ratio

$$\frac{\langle R^2\rangle_{2n}}{\langle R^2\rangle_n} \approx 2^{2\nu}(1+Cn^{-\Delta}) \tag{2.19}$$

should approach $2^{2\nu}$ in the expanded phase as $n\to\infty$. In the collapsed phase, a similar analysis suggests that the amplitude ratio should approach $2^{2/d}$; while ν gets replaced by the ν_θ, $\nu_{\theta'}$ and ν_p (whichever is appropriate) along the critical curve.

The mean perimeter. The mean perimeter of percolation clusters has received much attention in the literature (see for example, Stauffer 1979). If we define the partition function $\mathcal{Z}_n^p(p) = \sum_{c,k} a_n(c,k)p^n q^{s+k}$ for percolation, where $q = 1 - p$ and $P = s + k$ is the perimeter, then the expected value of P is given by

$$\langle P \rangle_p = \frac{q}{p} n + q \frac{\mathrm{d}}{\mathrm{d}q} \log \mathcal{Z}_n^p(p). \tag{2.20}$$

If we now assume the usual scaling for the partition function, $\log \mathcal{Z}_n^p(p) \sim \hat{h}(n^\sigma(p_c - p))$, where σ is the crossover exponent, then

$$\langle P \rangle_p \approx \frac{q}{p} n + Bn^\sigma \tag{2.21}$$

a relation that was tested numerically in Janse van Rensburg and Madras (1997). It is not evident that a similar relation applies along the line of θ-transition, and that the exponent σ is an exponent of tricritical θ-animals. We will present some data that σ can be seen away from the critical percolation point at the θ-points of collapse (see figure 7).

The mean branch size. We define the mean branch size of animals as follows (see Janse van Rensburg and Madras 1992, and Madras and Janse van Rensburg 1997). Let e be a cut-edge of an animal A. Then $A - e$ is disconnected, and the smaller of its two components is called a *branch*; let the size of the branch be b_n. The expected value of b_n is defined by taking the uniform average over all possible cut-edges in all animals. Let the exponent ϵ describe the scaling of $\langle b_n \rangle$:

$$\langle b_n \rangle \sim n^\epsilon \tag{2.22}$$

where $\epsilon \leqslant 1$. In the implementation of a cut-and-paste algorithm for animals it is more convenient to compute a related quantity. The algorithm selects an edge uniformly over all edges in the animal. If a cut-edge is not chosen, then we define the branch to have size zero. If a cut-edge is selected with probability p_n, then the observed size of a branch will be

$$\langle B_n \rangle \sim p_n \langle b_n \rangle + (1 - p_n).0 \sim p_n n^\epsilon. \tag{2.23}$$

We do not expect p_n to approach zero with increasing n in either the expanded phase or along the critical curve. In the collapsed phase the situation is less clear, but in a spanning tree regime we also expect p_n not to approach zero with increasing n. However, in the section graph regime, which results from collapse along the θ'-curve, we would presumably have compact animals rich in cycles, and p_n may approach zero.

3. Numerical results

We simulated lattice animals using the cut-and-paste algorithm for animals (Janse van Rensburg and Madras 1997). This algorithm was implemented with two techniques. In the first place, we used multiple Markov chain sampling to simulate animals (in the square lattice) along the axes of the phase diagram in figure 1. Secondly, we implemented the algorithm with an umbrella distribution over a rectangle $[0, 2\log 2] \times [0, 6\log 2]$ in the phase diagram which includes the critical curve in the first quadrant of figure 1.

3.1. Multiple Markov chain sampling

In this simulation we sampled along a set of parallel Markov chains in the state space of animals using a multiple Markov chain algorithm as explained in Tesi *et al* (1996). In the

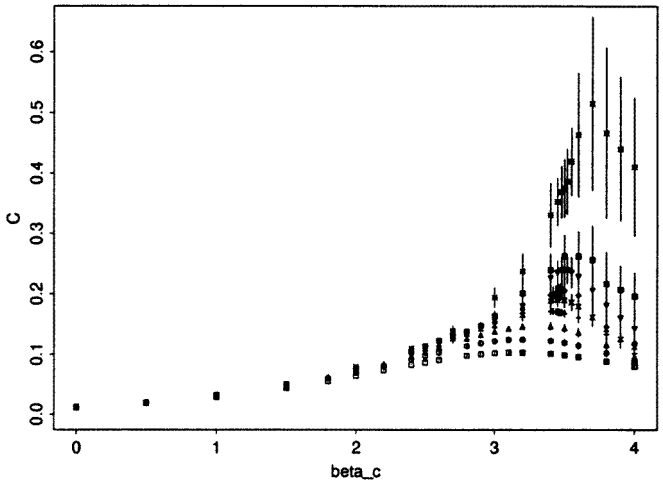

Figure 2. The specific heat as a function of the cycle fugacity, estimated using a multiple Markov chain Monte Carlo simulation. The data at $n = 50$ are indicated by squares, and the peaks systematically increase in height with n increasing in $\{50, 100, 200, 400, 800, 1200, 1600, 2400, 3200\}$.

first set of simulations, 20 parallel chains were placed along the $\beta_c = 0$ axis between $\beta_k = 0$ and $\beta_k = 2\log 2$ to simulate animals undergoing a contact collapse at a critical value of the contact fugacity β_k^*. In the second set of simulations, we placed 20 chains along the $\beta_k = 0$ axis between $\beta_c = 0$ and $\beta_c = 6\log 2$ to simulate animals undergoing a cycle collapse at the critical value β_c^* of the cycle fugacity. Our prime motive is the calculation of the crossover exponents ϕ_c and ϕ_k associated with the collapse transitions, as well as the location of the critical values β_k^* and β_c^*. In addition, we hope to obtain estimates of the metric exponents ν_θ and $\nu_{\theta'}$ at the critical points. Animals of sizes ranging from $n = 50$ to $n = 3200$ were sampled. The data for animals along the cycle axis are in figure 2.

The height and position of the peaks in the specific heat were estimated by interpolating the data collected from each chain. From equations (2.9) and (2.10) we conclude that the height in the peaks increases with n as

$$H_k(n) \sim n^{2\phi_k - 1} \qquad H_c(n) \sim n^{2\phi_c - 1} \tag{3.1}$$

while the position of the peak should move with n as

$$\beta_k(n) \sim \beta_k^* + \mathrm{O}(n^{-\phi_k}) \qquad \beta_c(n) \sim \beta_c^* + \mathrm{O}(n^{-\phi_c}). \tag{3.2}$$

We analysed our data using a least squares analysis†. Our results are

$$\begin{aligned} \phi_k &= 0.6027 \pm 0.0044 \pm 0.0071 \\ \phi_c &= 0.6274 \pm 0.0110 \pm 0.0010. \end{aligned} \tag{3.3}$$

The position of the collapse transition is extrapolated by using the values of ϕ_k and ϕ_c in equation (3.3), together with equation (3.2) to estimate β_k and β_c. The fits were repeated with

† A fit is deemed acceptable if the χ^2-statistic is acceptable at the 95% level. If a fit is not acceptable, then data at the smallest value of n (where corrections to scaling contribute the most) are discarded. We also estimate a systematic error by keeping track of our best estimate in a successful fit by discarding one more data point at the lowest value of n. The absolute difference in the results is taken as the systematic error. The statistical error will always be stated before the systematic error.

ϕ_k and ϕ_c taking values at the ends of their respective confidence intervals to estimate the effect of the uncertainty in these exponents on the location of the transition. Our best estimates are

$$\begin{aligned} \beta_k^* &= 0.719 \pm 0.076 \\ \beta_c^* &= 3.61 \pm 0.11 \end{aligned} \tag{3.4}$$

where the estimated systematic errors are much smaller than the stated 95% statistical confidence intervals. The estimated value for β_k^* compares well to the estimate 0.737 ± 0.015 obtained by exact enumeration (Peard 1995).

The mean square radius of gyration of the animals was also examined. The multiple Markov chain simulations each had a chain at zero fugacity, and those data can be used to obtain a high quality estimate of the metric exponent. If all the data are pooled, then a least squares analysis gives

$$\nu = 0.644\,19 \pm 0.000\,64 \pm 0.000\,31. \tag{3.5}$$

This result compares well with the estimates of ν for lattice trees and animals in the literature; it is more precise than the previous best Monte Carlo estimate (Janse van Rensburg and Madras 1992), and compares well with results obtained by other methods (Derrida and de Seze (1982) found $\nu = 0.6408 \pm 0.0003$ while Kertèsz (1986) estimated $\nu = 0.6406 \pm 0.0002$). We do not think that the difference of these estimates with our estimate is significant; there may still be other biases present in our data, or in those studies, which could account for the difference. The metric exponent at the contact collapse transition can be estimated by recording data at the peak in the specific heats. At the peak corresponding to the contact collapse, our best estimate is

$$\nu_\theta = 0.5191 \pm 0.0071. \tag{3.6}$$

On the other hand, we could not find a satisfactory two parameter fit to our data at the cycle collapse transition. Our 'best' estimate suggests that $\nu_{\theta'} \approx 0.52$, which is consistent with the result obtained in equation (3.6). At the percolation point $\nu_p = 0.532 \pm 0.005$ (Janse van Rensburg and Madras 1997), an estimate which is close to the estimate in equation (3.6). It seems that the available evidence does not rule out the possibility that ν assumes the same value all along the critical curve and at the percolation point in figure 1. If this is the case, then the critical percolation cluster and a θ-animal, or a θ'-animal, will have the same metric properties.

3.2. Umbrella sampling

The multiple Markov chain Monte Carlo implementation above collects data at a set of discrete values of the fugacities. There are several advantages in this approach, most notably the shortened autocorrelation times along the Markov chain, and the simultaneous collection of data at a number of different values of the fugacities. However, it would also be valuable to collect data over a region of parameter space; say over a rectangle which covers an area of interest in figure 1. This can be done using a variant of importance sampling called umbrella sampling (Torrie and Valleau 1977, Valleau 1991, 1993a). That this approach is appropriate in the model in this paper is suggested by the results obtained for collapsing lattice trees (Janse van Rensburg and Madras 1996, Madras and Janse van Rensburg 1997). The main difference in this work, compared to previous implementations, is that we aim to use umbrella sampling over a rectangle (involving two fugacities) rather than just along a line (which involves only one fugacity).

The implementation of the umbrella sampling scheme for animals proceeded as follows. Define A_n to be the set of all animals with n edges, and let α be such an animal. Let $c(\alpha)$

be the number of cycles and $k(\alpha)$ be the number of contacts in the animal α. The Boltzmann distribution P_n over the animals in A_n is given by

$$P_n(\alpha) = \frac{e^{\beta_c c(\alpha)+\beta_k k(\alpha)}}{Z_n(\beta_c, \beta_k)} \tag{3.7}$$

where $Z_n(\beta_c, \beta_k)$ is a normalizing function, and in this case is also the partition function defined in equation (2.1). In the usual implementation of the cut-and-paste Metropolis algorithm for animals, one samples along a Markov chain in A_n with limiting equilibrium distribution given by the Boltzmann distribution in equation (3.7). In this implementation, the animal α is weighted by the factor $e^{\beta_c c(\alpha)+\beta_k k(\alpha)}$. In the umbrella simulations we supposed that the animals are each assigned a weight $\pi(\alpha) = \pi(c(\alpha), k(\alpha))$, and let $Z_n(\pi) = \sum_\alpha \pi(\alpha)$. Then the Metropolis algorithm will have equilibrium probability distribution $\pi(\alpha)/Z_n(\pi)$ over the set A_n. Canonical averages can be computed using importance sampling techniques. Let f be a function on A_n, and define the following estimator over a chain of length m:

$$S_m(f) = \frac{1}{m}\sum_{i=1}^{m} \frac{f(X_i)}{\pi(X_i)} e^{\beta_c c(\alpha)+\beta_k k(\alpha)}. \tag{3.8}$$

The ratio estimator

$$R_m(f) = \frac{S_m(f)}{S_m(1)} \tag{3.9}$$

is a biased estimate of $\langle f\rangle_{\beta_c,\beta_k}$. An additional and important advantage is the ability to estimate relative free energies. The ratio estimator $S_m(1; \beta_c^{(2)}, \beta_k^{(2)})/S_m(1; \beta_c^{(1)}, \beta_k^{(1)})$ converges to $Z_n(\beta_c^{(2)}, \beta_k^{(2)})/Z_n(\beta_c^{(1)}, \beta_k^{(1)})$. By taking logarithms and dividing by n, we see that $\frac{1}{n}\log(S_m(1; \beta_c^{(2)}, \beta_k^{(2)})/S_m(1; \beta_c^{(1)}, \beta_k^{(1)})) \to F_n(\beta_c^{(2)}, \beta_k^{(2)}) - F_n(\beta_c^{(1)}, \beta_k^{(1)})$.

Obtaining an umbrella for a particular implementation can be a problem. The following method generally works, if it is used with patience. Assume that the umbrella distribution is a combination of Boltzmann distributions

$$\pi(\alpha) = \pi(c, k) = \sum_{i,j} w_{i,j} e^{\beta_c^{(i)} c(\alpha)+\beta_k^{(j)} k(\alpha)} \tag{3.10}$$

where the fugacities $\beta_c^{(i)}$ and $\beta_k^{(j)}$ form a grid over the rectangle of interest, and the Boltzmann factors are weighted by $w_{i,j}$ at each grid-point. Notice the implicit assumption that $\pi(\alpha)$ is only a function of the number of cycles and contacts. This is very convenient: we only need to construct a table of values of $\pi(c, k)$ in the implementation of the algorithm.

Since we wish to have an umbrella which will allow us to compute canonical averages at any of the grid points (say at $(\beta_c^{(i)}, \beta_k^{(j)})$), the contribution of that Boltzmann factor corresponding to this grid point should make a substantial contribution to (3.10). This is true for each i and j, which leads us to the following recipe: *adjust the weights $w_{i,j}$ such that each term in equation (3.10) makes a comparable contribution to $\pi(\alpha)$*. This means that

$$\langle\langle w_{i,j} e^{\beta_c^{(i)} c(\alpha)+\beta_k^{(j)} k(\alpha)}/\pi(c(\alpha), k(\alpha))\rangle\rangle_\pi \approx \langle\langle w_{k,l} e^{\beta_c^{(k)} c(\alpha)+\beta_k^{(l)} k(\alpha)}/\pi(c(\alpha), k(\alpha))\rangle\rangle_\pi. \tag{3.11}$$

In other words, we can solve for the ratios of the weights:

$$\frac{w_{i,j}}{w_{k,l}} \approx e^{n(F_n(\beta_c^{(k)},\beta_k^{(l)}) - F_n(\beta_c^{(i)},\beta_k^{(j)}))} \tag{3.12}$$

where we used $F_n(\beta_c, \beta_k) = [\log Z_n(\beta_c, \beta_k)]/n$. Thus, if we know the free energies, then we can find a good umbrella. Unfortunately, this is a circular argument; in order to find good estimates of the free energies, we need a good umbrella in the first place. All is not lost, however, as we boot-strapped our simulations by starting at a small value of n, and estimated

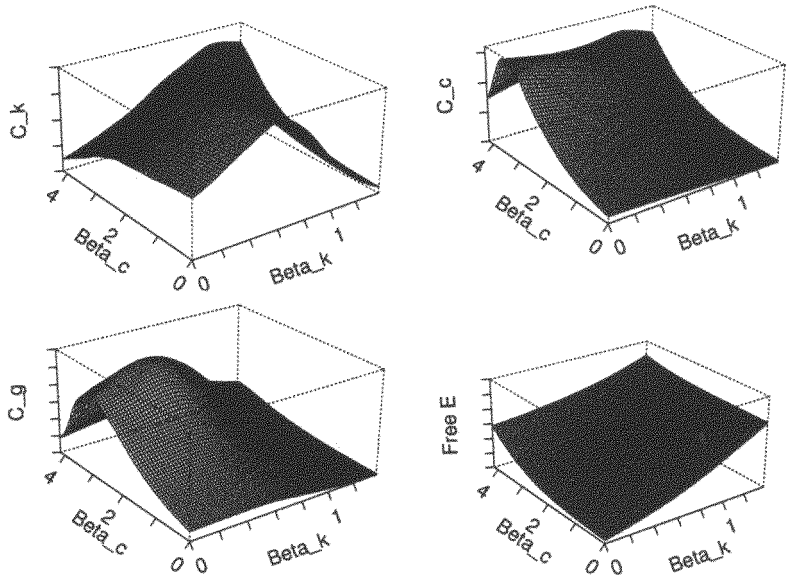

Figure 3. The estimated specific heats and free energy, obtained from the umbrella Monte Carlo simulation. Clockwise from the top left-hand corner we have C_n^{kk}, C_n^{cc}, $\mathcal{F}(\beta_k, \beta_c)$ and C_n^g.

the free energies over a 100×100 grid covering the rectangle $[0, 2\log 2] \times [0, 6\log 2]$. The results were then used to estimate weights at a larger value of n. If the resulting weights did not give a good umbrella, then we repeated the run with new weights estimated from the results of the previous run. This technique consistently gave a good umbrella after a few iterations, at the expense of considerable computer time! Finally, the resulting time series from a run with a good umbrella were analysed over a 70×70 grid which covers the rectangle $[0, 2\log 2] \times [0, 6\log 2]$. Animals of size n were sampled in these runs once every n iterations, and for animals of size up to 400 edges we sampled 10^6 times (the total run had length $10^6 n$ iterations). For animals of size 500 we sampled data 1.2×10^6 times, and for animals of sizes 600 and 800 we sampled data 2×10^6 times. The total CPU time used ran into weeks for larger values of n.

3.2.1. Specific heats. We computed C_n^{kk} and C_n^{cc} as in equations (2.9) and (2.10) by collecting data on the number of cycles and contacts in the animals. In addition, the Gaussian curvature of the free energy (equation (2.15)) was also computed. In figure 3 we illustrate these specific heats for animal of size $n = 300$ over the sampling area.

We estimated the height and the location of the peak in the specific heat C_n^{kk} along the contact axis to estimate the exponent ϕ_k in equations (2.9) and (3.1). Linear least squares analysis, using the same criteria as in section 3.1, gave the estimate

$$\phi_k = 0.622 \pm 0.009 \pm 0.022 \tag{3.13}$$

of the crossover exponent associated with contact collapse in animals. The critical value of the contact fugacity can also be estimated, assuming that equation (3.2) applies here. We obtained

$$\beta_k^* = 0.711 \pm 0.11 \pm 0.08. \tag{3.14}$$

We similarly analysed the data computed from the specific heat C_n^{cc} along the cycle axis to estimate the crossover exponent associated with cycle collapse, and the critical value of the

cycle fugacity at this collapse. We obtained

$$\phi_c = 0.622 \pm 0.006 \pm 0.026 \tag{3.15}$$

$$\beta_c^* = 3.52 \pm 0.032 \pm 0.010. \tag{3.16}$$

These results are consistent with the values obtained from the (independent) multiple Markov chain Monte Carlo method, and stated in equations (3.3) and (3.4).

The height of the peak in the Gaussian curvature of the free energy was argued to increase with n as in equation (2.16). From equation (2.15), and by using (2.9) and (2.10), it seems that a reasonable scaling assumption for the peak in C_n^g is

$$C_n^g(\beta_c, \beta_k) \sim n^{2(\phi_c+\phi_k)-2}\hat{h}(n^{\phi_c}\kappa, n^{\phi_k}\chi) \tag{3.17}$$

where $\hat{h}$ is a universal scaling function. In other words, the location of the peak should scale with n as

$$\begin{aligned} \beta_c(n) &= \beta_c^* + \mathrm{O}(n^{-\phi_c}) \\ \beta_k(n) &= \beta_k^* + \mathrm{O}(n^{-\phi_k}). \end{aligned} \tag{3.18}$$

In addition, we expect the limiting position of the peak to coincide with the percolation point in figure 1. A least squares analysis gives

$$\begin{aligned} \beta_k^* &= 0.60 \pm 0.30 \\ \beta_c^* &= 3.54 \pm 0.30. \end{aligned} \tag{3.19}$$

The large error bars are rounded (up) statistical uncertainties. These results can be used to compute the critical percolation probability as an additional check. From $\beta_k = 0.60$ and equation (2.7) we obtain $p_c \approx 0.45$ and from $\beta_c = 3.54$ we obtain $p_c \approx 0.587$, both estimates with large error bars. A more successful approach is found if we plot the peaks in the Gaussian curvature against p. This gives $p_c = 0.491 \pm 0.008$, which is consistent with the known value of p_c. The exponent $2(\phi_c + \phi_k) - 2$ in equation (3.17) can also be determined by analysing the height of the Gaussian curvature of the free energy. We obtained

$$2(\phi_c + \phi_k) - 2 = 0.4019 \pm 0.17 \pm 0.01. \tag{3.20}$$

This result is consistent with the estimates of ϕ_k and ϕ_c in equations (3.13) and (3.15).

3.2.2. The mean square radius of gyration. We collected data on the mean square radius of gyration for uniformly weighted animals (these are at the origin in figure 1), and for animals weighted as θ-animals (at the point $(0, \beta_k^*)$ on the contact axis), and weighted as θ'-animals (at the point $(\beta_c^*, 0)$ on the cycle axis) and as critical percolation clusters. We estimated the metric exponent ν at each of these points:

$$\begin{aligned} \nu &= 0.6476 \pm 0.0037 \pm 0.0006 \\ \nu_\theta &= 0.5364 \pm 0.0033 \pm 0.0021 \\ \nu_{\theta'} &= 0.5546 \pm 0.0039 \pm 0.0009 \\ \nu_p &= 0.5335 \pm 0.0031 \pm 0.0036. \end{aligned} \tag{3.21}$$

The estimate of ν for expanded animals is consistent with other estimates in the literature (Janse van Rensburg and Madras 1997). The value estimated for ν_p is also consistent with the accepted value for critical percolation, which is approximately 0.53. The estimate for θ-animals is consistent with this value, but we note that our result for θ'-animals excludes both the values of the metric exponent for critical percolation clusters and θ-animals with the stated error bars. Most available data (see for example, Derrida and Hermann 1983, Madras and Janse van Rensburg 1997, Janse van Rensburg and Madras 1997) suggest that θ- and θ'-animals have

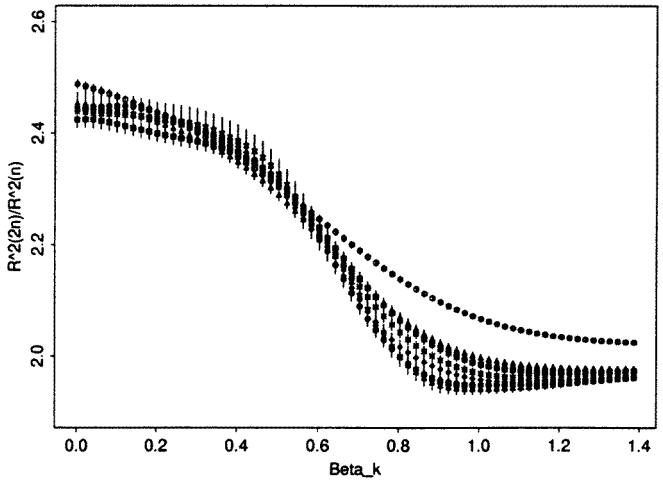

Figure 4. Amplitude ratios of the mean square radius of gyration against β_k.

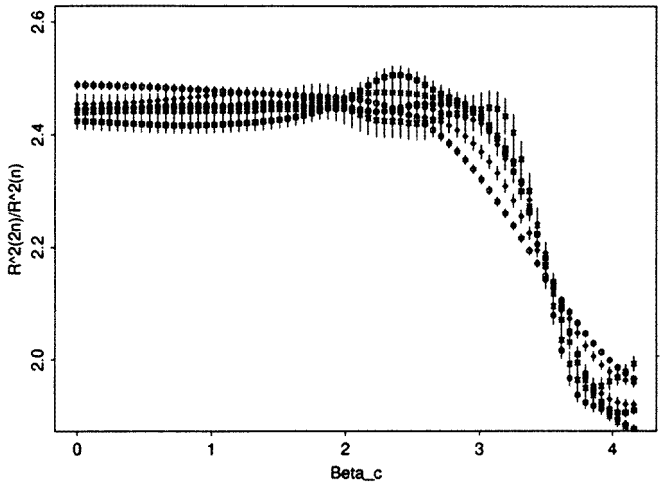

Figure 5. Amplitude ratios of the mean square radius of gyration against β_c.

a metric exponent close in value to critical percolation clusters, and our data does not suggest otherwise (it is still possible that there is an unknown systematic error in the estimates above, which we cannot detect by our analysis; for more on this possibility, see You and Janse van Rensburg (1998)).

Amplitude ratios of the mean square radius of gyration were also computed along the contact, and cycle fugacity axes in figure 1. We illustrate those in figures 4 and 5. The inflection points in the amplitude ratios may be taken as estimates of the collapse transitions. If we extrapolate the inflections in figure 4, then we obtain the estimate $\beta_k^* \approx 0.71$, which is consistent with the estimates obtained from the specific heat data above in equation (3.14). Similarly, we can extrapolate the inflections in figure 5 to obtain the estimate $\beta_c^* \approx 3.52$, which is also consistent with the result we obtained by considering the specific heat data. Finally, the amplitude ratios can also be plotted against p along the percolation line in figure 1. The

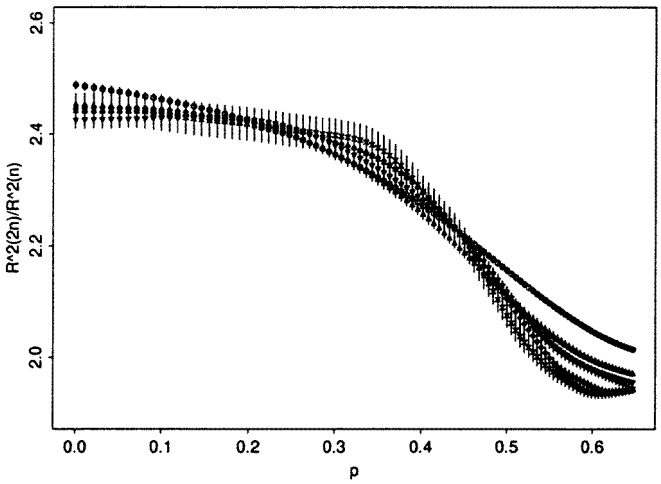

Figure 6. Amplitude ratios of the mean square radius of gyration against p along the percolation line.

resulting curves are plotted in figure 6. The metric collapse in these ratios should coincide with percolation in the clusters, and the inflection points in each curve should be estimating the critical value of p. An average over the inflection points gives 0.45 ± 0.02.

3.2.3. The mean perimeter. Data on the mean perimeter were also collected for expanded animals at the origin in figure 1, as well as at the critical points on the contact axis, the cycle axis, and at the critical percolation point. For expanded animals, the perimeter should grow as n, and by assuming that $\langle P_n \rangle = An^{\omega}$, a least squares analysis of our data gives

$$\omega = 0.9922 \pm 0.0017 \pm 0.0013. \tag{3.22}$$

At the percolation point, the behaviour of $\langle P_n \rangle$ should be given by equation (2.21). Since $p_c = \frac{1}{2}$, we can estimate the percolation crossover exponent σ in (2.21). A linear least squares analysis gives

$$\sigma = 0.3861 \pm 0.0042 \pm 0.0023. \tag{3.23}$$

It is more difficult to estimate the dependence of the mean perimeter on n at the θ- and θ'-transitions along the axes in figure 1. Equation (2.21) suggests that $\langle P_n \rangle \approx An + Bn^{\sigma}$; if it is true that the exponent σ exists away from the critical percolation point. We tested this asssumption in figure 7 by plotting $\langle P_n \rangle / n$ against $n^{\sigma - 1}$. The resulting plots are linear, and confirms the notion that σ describes the surface contribution to the perimeter for critical animals along the critical curve in figure 1.

The perimeter of an animal should change as it goes through a collapse transition to a compact animal. The plots in figure 7 suggests that

$$\frac{\langle P_n \rangle}{n} \approx \psi(\beta_c, \beta_k) + Bn^{\sigma - 1} \tag{3.24}$$

where ψ is an amplitude. We investigated the function ψ along the contact and cycle axis by plotting $\langle P_n \rangle / n$ against β_k and against β_c in figures 8 and 9. The inflection point in ψ should again be an estimate of the critical points: we found that $\beta_k^* \approx 0.73$ and $\beta_c^* \approx 3.45$ by extrapolating the inflection points in figures 8 and 9. These results are not inconsistent with our previous results.

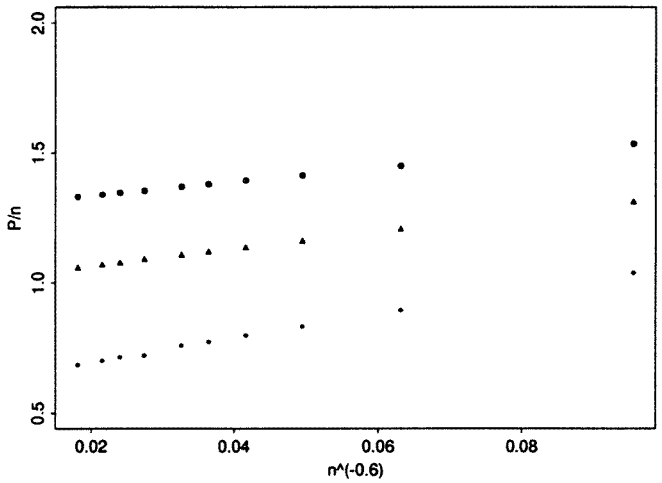

Figure 7. The density of perimeter edges in the animal plotted against $n^{\sigma-1}$. The data points represented by $\circ$ were obtained at $(\beta_k^*, 0)$; those represented by $\bullet$ were obtained at $(0, \beta_c^*)$; and those represented by $\triangle$ were obtained at the critical percolation point.

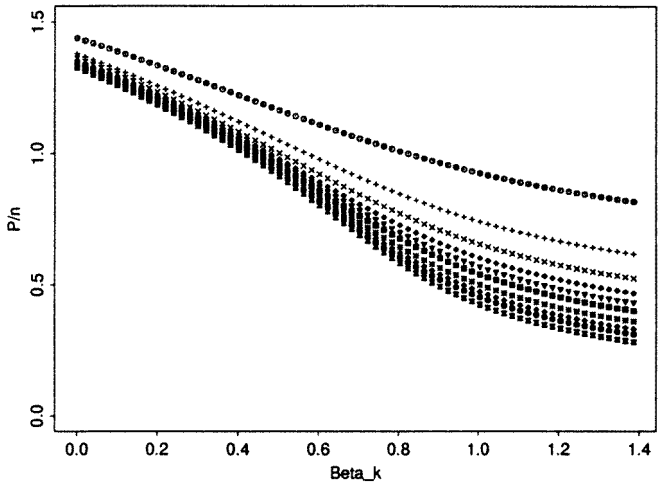

Figure 8. P_n/n against β_k along the contact axis. We expect this to approach a limiting curve. The value of n increases systematically from top to bottom.

The ratio P_n/n can also be computed along the percolation line and plotted as a function of the percolation probability p. The inflection points in these curves should converge to the critical value of p with increasing n. Our results are shown in figure 10, and the average of the inflection points estimates that $p_c = 0.514 \pm 0.018$, in close agreement with the known value of $p_c = \frac{1}{2}$.

3.2.4. The mean branch size. Data were similarly collected for the mean branch size for expanded animals, and for θ- and θ'-animals and for critical percolation clusters. The exponent

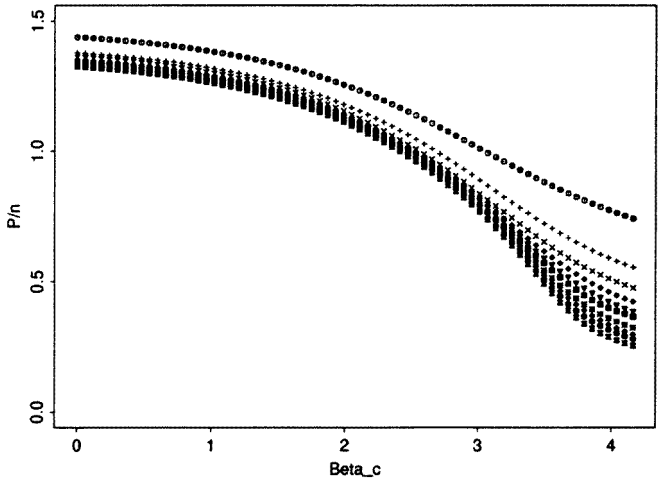

Figure 9. P_n/n against β_c along the cycle axis. We expect this to approach a limiting curve. The value of n increases systematically from top to bottom.

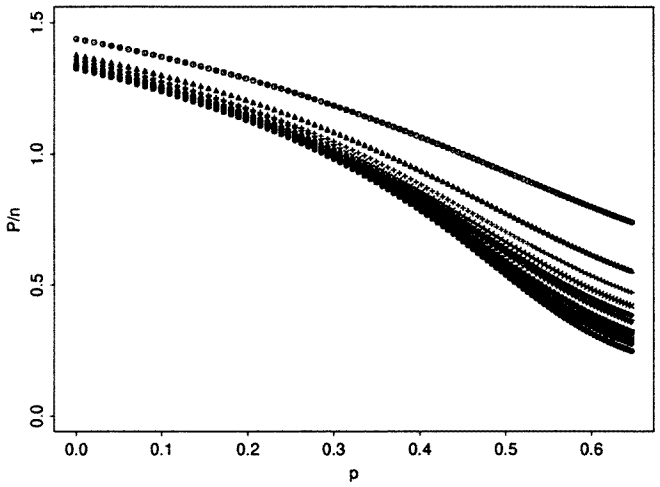

Figure 10. P_n/n against p along the percolation line. We expect this to approach a limiting curve. The value of n increases systematically from top to bottom.

ϵ was estimated in each case as

$$\begin{aligned}\epsilon &= 0.7447 \pm 0.0100 \pm 0.0013\\ \epsilon_\theta &= 0.6665 \pm 0.0110 \pm 0.0056\\ \epsilon_{\theta'} &= 0.031 \pm 0.042 \pm 0.017\\ \epsilon_p &= 0.427 \pm 0.018 \pm 0.013.\end{aligned} \tag{3.25}$$

In this case we obtained different values for each regime. The estimate for expanded animals coincide with the estimate in Janse van Rensburg and Madras (1997), as does the estimate at the critical percolation point. The value estimated for θ-animals are different, suggesting larger branches (on average) in the animals. The exponent has a very small estimated value for θ'-animals. These animals have a lot of cycles, and the result suggests that deleting a cut-edge

in such an animal is likely to give a small branch. The opposite is true for percolation clusters, where a larger value of ϵ_p is found: if a cut-edge is deleted, then we can expect, with some probability, a large branch (in other words, most cycles are small).

We have also made an attempt to estimate the exponent ϵ in the collapsed phase. At the point $\beta_k = 1$, $\beta_c = 0$ (this is on the contact axis, well into the collapsed phase), a least squares analysis gives

$$\epsilon_k = 0.659 \pm 0.011 \pm 0.010. \tag{3.26}$$

The fit was good with $\chi^2 \approx 2$ on eight degrees of freedom at $n_{min} = 50$. Remarkably, the value of ϵ obtained here is within the error bars of ϵ_θ in equation (3.25). Thus, it seems that there is no further change in the branching characteristics of the lattice trees if we move beyond the θ-line into the collapsed phase. On the other hand, if we consider the data on the cycle axis in the collapsed phase at $\beta_k = 0$, $\beta_c = 4$, then we are unable to determine an exponent. In fact, the mean branch size *declines* with increasing n; and this observation suggests that either $\epsilon = 0$, or that there are no small branches in the animal which grows with n.

4. Conclusions

In this paper we examined the phase diagram of a model of self-interacting lattice animals on the square lattice. The model we studied has both a contact and a cycle fugacity, and increases in either of these fugacities (with the other fixed) will take the animal through a θ-point into the collapsed phase. We set out to compare the collapse transitions induced by either the contact or by the cycle fugacities numerically, using Monte Carlo techniques, and by estimating critical exponents associated with the transitions. In the first place we have used a multiple Markov chain Monte Carlo simulation with two sequences of fugacities along the axes in figure 1. We estimated the crossover exponents associated with contact collapse and with cycle collapse in equation (3.3), and the locations of the critical points in equation (3.4). The results for contact collapse are consistent with earlier results obtained for collapsing lattice trees (Janse van Rensburg and Madras 1996).

The values of the two crossover exponents, ϕ_c and ϕ_k, obtained from the multiple Markov chain Monte Carlo sampling are different, and points towards the possibility that the contact collapse and cycle collapse in this model may be characterized by different exponents. The estimated value of $\phi_c \approx 0.63$ for cycle collapse is lower than the estimate of 0.66 by Derrida and Hermann (1983) (see also, Seno and Vanderzande 1994a, b). Our results from the umbrella sampling simulations are more ambivalent as far as the crossover exponents are concerned. Indeed, our best values estimated in equations (3.13) and (3.15) coincide, but since the estimated error bars are relatively large, they are not inconsistent either with the results from the multiple Markov chain Monte Carlo, or with the simulations of collapsing trees (Janse van Rensburg and Madras 1996). The estimated locations of the critical points are once again consistent with previous results. In particular, the location of the critical point for contact collapse at $\beta_k^* \approx 0.72$ is consistent with the conjecture that the critical curve of contact-collapse transitions (the θ-line in figure 1) is a straight line, made in an earlier study of lattice animals (Janse van Rensburg and Madras 1997). From this point of view the critical curve in figure 1 is non-analytic at the critical percolation point. This suggests that the percolation point is a multicritical point on the critical curve, separating two lines of collapse transitions which are in different universality classes. An alternative point of view is suggested by the results in figure 7. In this case we note that the percolation perimeter exponent σ seems to be also the perimeter exponent of θ- and θ'-animals. This result indicates the possibility that collapse in animals is in the critical percolation universality class. In this case there is a single curve of critical percolation points

in figure 1. The estimates of the metric exponents in equation (3.21) is consistent with this view as well, and is also consistent with the results obtained for lattice trees (Janse van Rensburg and Madras 1996). The estimate along the cycle collapse is slightly larger, but we cannot rule out the possibility that an increase in the size of the animals, and longer simulations, will give a result equal to the percolation value. The value of the percolation perimeter (crossover) exponent is consistent with previous estimates (Stauffer 1979, Janse van Rensburg and Madras 1997).

Amplitude ratios of the mean square radius of gyration, and of the mean perimeter supports the notion of universality in this problem, and inflection points in these are consistent with the estimated critical points. The mean branch size does indicate the existence of different regimes (if not phases) in this model. In particular, the estimates in equation (3.25) assigns different values of this exponent along the contact-collapse line, the percolation point, and the cycle-collapse curve. Moreover, in the collapsed regime, we also estimated ϵ: along the contact axis we obtained the same value as at the θ-point for contact collapse, but along the cycle axis it seems that this exponent is equal to zero. The different values of the exponent ϵ suggest that the dominant configurations at the two θ-points are geometrically different. This does not mean that there is a transition between these regimes, but rather a geometric crossover from one class of θ-transitions to the other. The fact that $\epsilon = 0$ along the cycle collapse line is also reflected in the fact that the collapsed cycle animal (albeit in a different ensemble) has zero entropy, see Madras *et al* (1990) for more on this.

Acknowledgments

The authors acknowledge numerous discussions with S G Whittington. EJJvR is supported by NSERC (Canada) operating and equipment grants.

References

Chang I S and Shapir Y 1988 *Phys. Rev.* B **38** 6736
Coniglio A, Jan N, Majid I and Stanley H E 1987 *Phys. Rev.* B **35** 3617
de Gennes P G 1975 *J. Physique Lett.* **36** L55
——1978 *J. Physique Lett.* **39** L299
Derrida B and de Seze L 1982 *J. Physique* **43** 475
Derrida B and Herrmann H J 1983 *J. Physique* **44** 1365
Dickman R and Schieve W C 1984 *J. Physique* **45** 1727
——1986 *J. Stat. Phys.* **44** 465
Duplantier B 1986 *Europhys. Lett.* **1** 491
——1987 *J. Chem. Phys.* **86** 4233
Duplantier B and Saleur H 1987 *Phys. Rev. Lett.* **59** 539
Flesia S and Gaunt D S 1992 *J. Phys. A: Math. Gen.* **25** 2127
Flesia S, Gaunt D S, Soteros C E and Whittington S G 1992a *J. Phys. A: Math. Gen.* **25** 3515
——1992b *J. Phys. A: Math. Gen.* **26** L993
Gaunt D S and Flesia S 1990 *Physica* A **168** 602
——1991 *J. Phys. A: Math. Gen.* **24** 3655
Geyer C J and Thompson E A 1994 *J. Am. Stat. Assoc.* **90** 909
Grimmett G 1989 *Percolation* (New York: Spinger)
Hammersley J M and Handscomb D C 1964 *Monte Carlo Methods* (London: Metheun)
Henkel M and Seno F 1996 *Phys. Rev.* E **53** 3662
Janse van Rensburg E J and Madras N 1992 *J. Phys. A: Math. Gen.* **25** 303
——1996 *Numerical Methods for Polymeric Systems, Proc. 1995/96 IMA program on Mathematical Methods in Material Science, Workshop 7 (May, 1996)* ed S G Whittington
——1997 *J. Phys. A: Math. Gen.* **30** 8035
Kertèsz J 1986 *J. Phys. A: Math. Gen.* **19** 599

Lam P M 1987 *Phys. Rev.* B **36** 6988
——1988 *Phys. Rev.* B **38** 2813
Madras N and Janse van Rensburg E J 1997 *J. Stat. Phys.* **86** 1
Madras N, Soteros C E, Whittington S G, Martin J L, Sykes M F, Flesia S and Gaunt D S 1990 *J. Phys. A: Math. Gen.* **23** 5327
Mazur J and McCrackin F L 1968 *J. Chem. Phys.* **49** 648
Mazur J and McIntyre D 1975 *Macromolecules* **8** 464
Metropolis N, Rosenbluth A W, Rosenbluth M N, Teller A H and Teller E 1953 *J. Chem. Phys.* **21** 1087
Park I H, Kim J H and Chang T 1992 *Macromolecules* **25** 7300
Peard P 1995 *PhD Thesis* King's College, London
Saleur H 1986 *J. Stat. Phys.* **45** 419
Seno F and Vanderzande C 1994a *J. Phys. A: Math. Gen.* **27** 5813
——1994b *J. Phys. A: Math. Gen.* **27** 7937
Stauffer D 1979 *Phys. Rep.* **54** 1
Sun S F 1990 *J. Chem. Phys.* **93** 7508
Sun S T, Nishio I, Swislow G and Tanaka T 1980 *J. Chem. Phys.* **73** 5971
Tesi M C, Janse van Rensburg E J, Orlandini O and Whittington S G 1996 *J. Stat. Phys.* **82** 155
Torrie G M and Valleau J P 1977 *J. Comput. Phys.* **23** 187
Valleau J P 1991 *J. Comput. Phys.* **96** 193
——1993 *J. Chem. Phys.* **99** 4718
You S and Janse van Rensburg E J 1998 *Phys. Rev.* E **58** 3971